

Notable mechanical behavior of thin monoholar rubber flat slab under tension loading

Kulyuth Boonseng*¹⁾, Chatchai Waiyapattanakorn²⁾ and Prayoon Surin¹⁾

¹⁾Faculty of Engineering, Pathumwan Institute of Technology (PIT), Bangkok 10330, Thailand

²⁾Independent Academic, Bangkok 10210, Thailand

Received 3 March 2020

Revised 15 May 2020

Accepted 28 May 2020

Abstract

There have been strong interests in achieving unconventional mechanical properties of materials utilized for various applications in recent years. Apart from the well known composite material approach, an innovative approach of employing cellular structure or repeated geometric pattern has been of great interest. The simple example that has been proved useful and promising is the monoholar pattern. Experimental investigations of monoholar rubber flat slab have demonstrated a number of unusual mechanical behaviors under compression loading unable to achieve before. It is thus enticing to find out if the same is possible under tension loading. This research therefore embarks on applying tension load on a thin monoholar rubber flat slab, 1/10 as thick as the flat slab tested under compression loading. Results of the experiments clearly demonstrate similar behaviors as observed in the case of compression loading. However stress plateau is not observable in the stress-strain curve obtained under tension loading. This is because the test specimen reaches rupture point after undergoing a certain level of stress. Ligament thickness has been observed to effect noticeable drop in stress level before gradually increasing towards stress level that causes full blown rupture. This may lead to some promising applications related to tension loading.

Keywords: Mechanical behaviors, Thin monoholar, Solid material, Tension loading

1. Introduction

Over the past three decades, there have been developments that lead to extraordinary mechanical behavior of a novel type of materials [1-3]. This novel type of materials could unleash tremendous potential in various areas of applications. Recent advancements of manufacturing technique have sparked great interest in this type of materials. The trick that makes possible a number of extraordinary mechanical behaviors is the so called cellular structure or the repeated geometric pattern. An example of such an idea is the monoholar rubber flat slab. The studies of the cellular structure offer new insights into the fabrication of novel materials and devices with tailored properties. The cellular structures of materials with their special mechanical and physical properties play an important role in determining their properties [4-9]. The benefits that arise from cellular structure are various unpredictable properties with multifunctionalities that could not be achieved in conventional materials [8, 10-13].

It is well known that the physical characteristics of the material affect its mechanical properties of the material, even when using the same chemical composition [6, 13-16]. The changes in structural patterns at macroscale can be triggered by elastic instability at the macroscale [6-7]. Thus cellular structure materials' functionality relies on elastic instabilities, such as the quasi-2D slabs perforated with a square array of holes [6, 8, 17-20]. These materials have since been widely applied in the development of novel products, useful in the automotive, defense, sport, aerospace, energy industries [14, 20-23], shape memory foams, and bioprostheses [20, 24-25]. Certain

applications related to compression loading and tension loading are running shoes, helmets, auto parts [20-21], aerospace [22-24] etc.

This paper focuses on some notable mechanical behaviors of thin monoholar rubber flat slab under tension loading. This is because the monoholar pattern is simple and exhibiting the highest stiffness [19]. There have been a number of published reports on the behavior of much thicker monoholar rubber flat slab under compression loading, but little or none on tension loading has been reported. In compression loading experiments emphasis is on mechanical behavior during the early stage of loading. [6, 8, 26-29], Increasing the ligament thickness, the loop size is larger and the stress increased. [8] Only hysteretic characteristics and stress-strain curves are of concern herein. Therefore two loading actions are to be performed, the cyclical tension applications and beyond rupture tension loading. Ligament thickness is a parameter of interest in this work.

2. Experimentation

This section describes both the specimen preparation and experimental setup. The experiments to be performed are those of tension loading actions on both the solid flat slab (SFS) (the referenced specimen) and the monoholar flat slab (MFS) (the investigated specimen). Both types of specimens are made of compounded rubber. Specimen preparation is to be described first then detail of the experimental setup is given succinctly.

2.1 Specimen preparation

*Corresponding author. Tel.: +6681 690 9286

Email address: Kulyuth.bo@skru.ac.th

doi: 10.14456/easr.2021.1

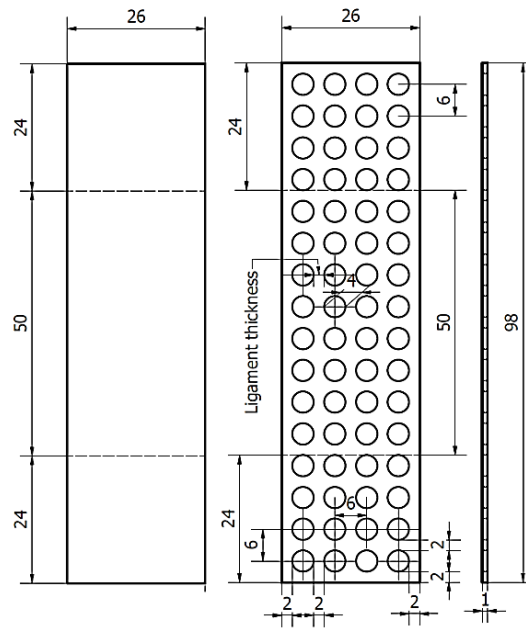


Figure 1 Specimen geometries model 1 (a) M1-SFS (b) M1-MFS

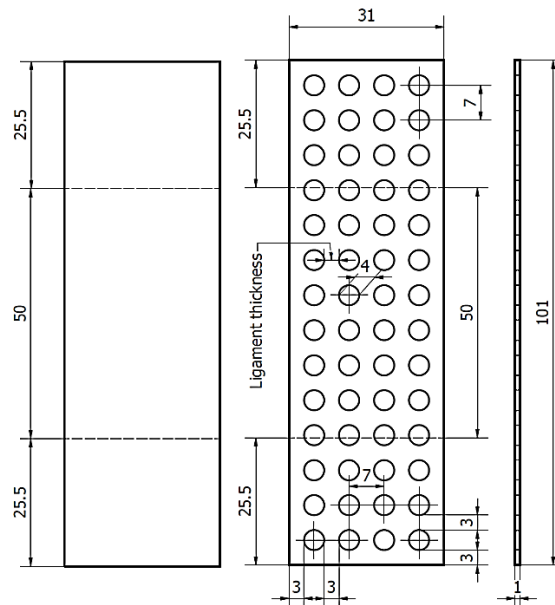


Figure 2 Specimen geometries model 2 (a) M2-SFS (b) M2-MFS

This research has opted for a compounded rubber made of Standard Thai Rubber (STR20) 40 phr, Butadiene Rubber 60 phr, silica 50 phr and other compounds used in the shoe industry. The cellular structure of interest herein is the monoholar array. This is because of its construction simplicity [26]. Figures 1-3 depict geometries of both the solid and monoholar flat slabs employed in the experiment. Both specimens are different in physical structure at the macro level. They are labelled as Model 1(M1) Model 2 (M2) and model 3(M3) as shown in Figures 1-3 respectively. All dimensions are in millimeter. It is evident from all 3 figures that ligament thickness, a parameter of interest in this work, has been varied from 2-4 mm. Both types of flat slabs are 1 mm thick. They are hence thin flat slabs. This is very interesting under tension loading. Specimens preparation has been carried out as illustrated in Figure 4.

2.2 Experimental setup

Tensile properties are to be tested uniaxially using a universal testing machine (UTM), Narin Universal Testing Machine Model

NRI-T500-20B. The uniaxial tensile test is a standard procedure for gauging hyperelastic properties [30]. Hysteretic characteristics are to be observed by pulling the specimens to 100 percent elongation, then the specimen is allowed to shrink back to its initial state (cyclic loading and unloading) [31]. Stress-strain curve can be drawn by observing stress-strain characteristics when pulling the specimen to rupture point at the rate of 500 mm / min at room temperature ($25 \pm 2^\circ \text{C}$) according to ASTM D412. 5 specimens are to be tested and results are averaged to yield a reported value.

3. Results and discussion

The experiments performed as stated in section 2 yield a number of notable results for both the hysteretic characteristics and the stress-strain curves. What have been observed for the MFS can be markedly distinguished from those of the SFS. Certain details and discussion of both aspects of the experiments are as follows.

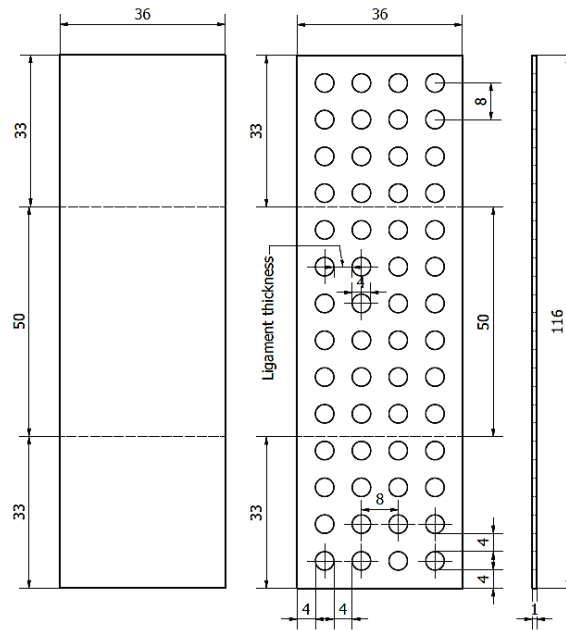


Figure 3 Specimen geometries model 3 (a) M3-SFS (b) M3-MFS

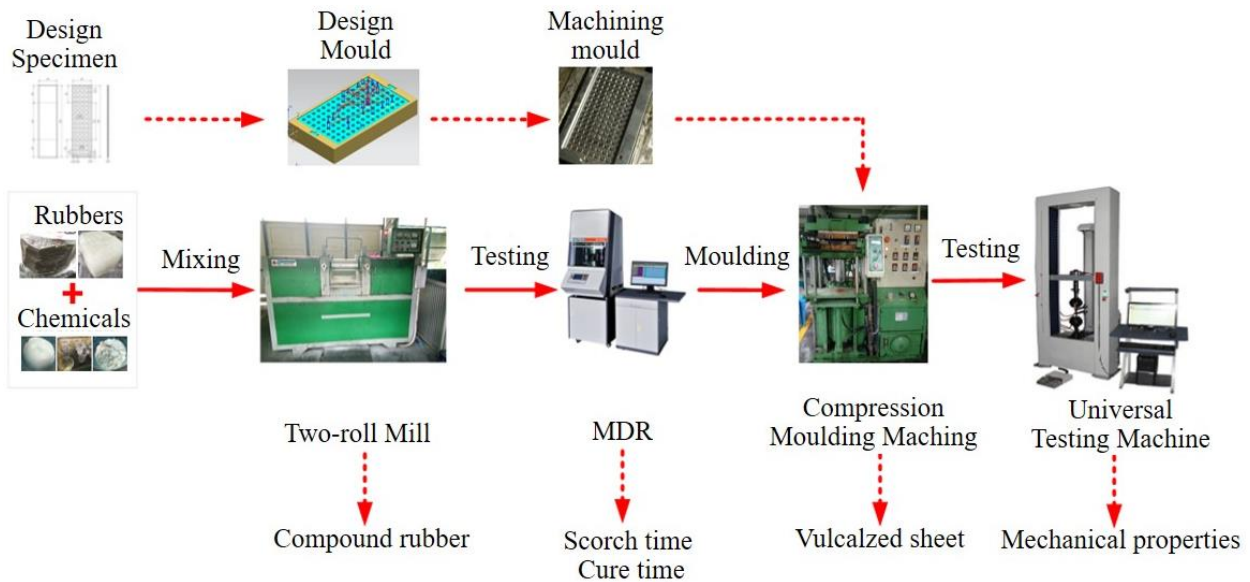


Figure 4 Specimens preparation process

3.1 Hysteretic characteristics due to cyclic Loading and unloading

Hysteretic characteristics of both the MFS and SFS of all models are shown in Figures 5-7. It can be seen that the MFS is capable of withstanding greater stress compared with the SFS under the same strain level. The hysteresis loops of the monoholar cases also appear significantly larger than the solid cases, a phenomenon also seen in compression loading experiment [32]. This is likely due to elastic instability caused by the presence of the circular hole array in the MFS [6]. This elastic instability makes the difference between the pulling stress and the retracting stress become larger, thus resulting in a larger hysteresis loop. The hysteresis loops of MFS are large, showing a significant loss of energy resulting in better energy absorption than SFS. In addition ligament thickness does alter the tolerable stress level and also the loop size. Greater ligament thickness reduces tolerable stress level and hence smaller hysteresis loop (Figures 5-7). The effect of increasing the ligament thickness tends to decrease the size of the loop, showing the ability to see

the lower energy lining as well. As opposed to under compression loading when increasing the ligament thickness, resulting in the loop size is larger. [8]. Also the MFS in this research is thin which is likely to undergo greater elastic instability. The larger hysteresis loop of the MFS does not make it unable to get back to the same state as that of the SFS when completely unloaded from the same level of tensile strain. However both types of flat slabs do not return to their initial state before applying tension loading [33]. The energy loss arising from the difference of the absorbing and releasing heat is a result of the viscoelastic properties of rubber. [34]

3.2 Stress-strain curve under tension loading to the rupture point

Figures 8-10 show that all 3 models of the MFS can be elongated to approximately 200% of their initial lengths, but the thin SFS can be pulled to be stretched to more than 400% of their initial lengths, more than double that of the MFS. At the same strain level the MFS withstand greater stress compared with the SFS. This means greater stiffness to tension loading for moderate

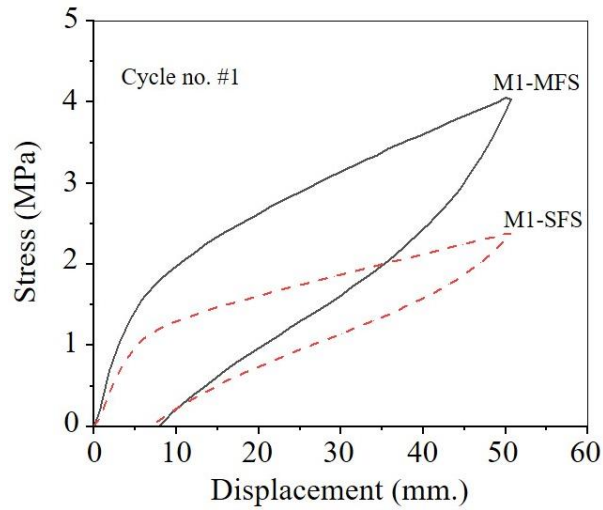


Figure 5 Hysteretic characteristics under tension loading and unloading of M1-MFS and M1-SFS

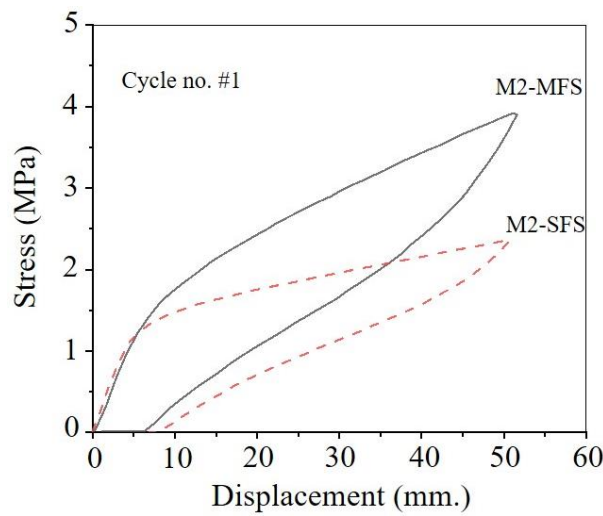


Figure 6 Hysteretic characteristics under tension loading and unloading of M2-MFS and M2-SFS

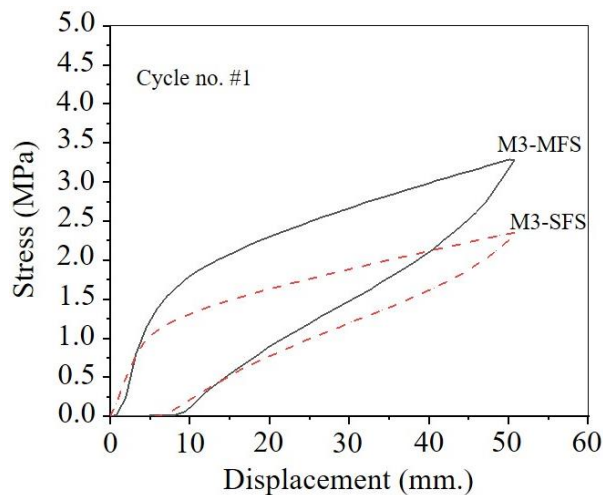


Figure 7 Hysteretic characteristics under tension loading and unloading of M3-MFS and M3-SFS

level of loading, a phenomenon also observed under compression loading [35-36]. This is also likely due to elastic instabilities and therefore they are reversible and repeatable of the MFS [6, 8]. At rupture points of both specimens for model 1, the MFS specimen undergoes slightly higher stress than the SFS specimen. When ligament thickness increases, models 2 and 3, rupture point stress

levels drop noticeably, as shown in Figures 9 and 10. When considering elastic behavior all models of MFS specimens appear superior. Ligament thickness also plays a role in increasing strain level that linear elasticity can sustain. All SFS specimens appear linearly elastic up to a strain level of about 9.0%, whereas the three MFS specimens appear linearly elastic upto about 11%

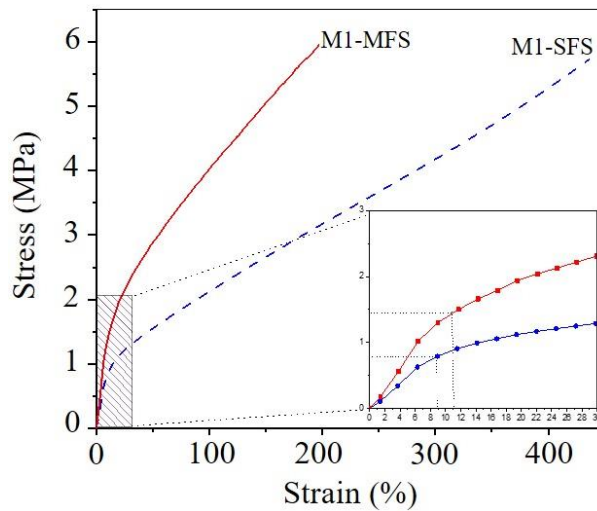


Figure 8 Stress-strain curves of the M1-MFS and M1-SFS under tension loading to the rupture point.

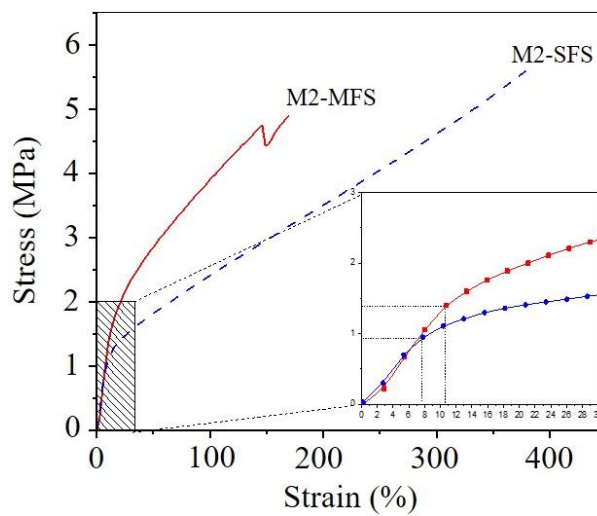


Figure 9 Stress-strain curves of the M2-MFS and M2-SFS under tension loading to the rupture point.

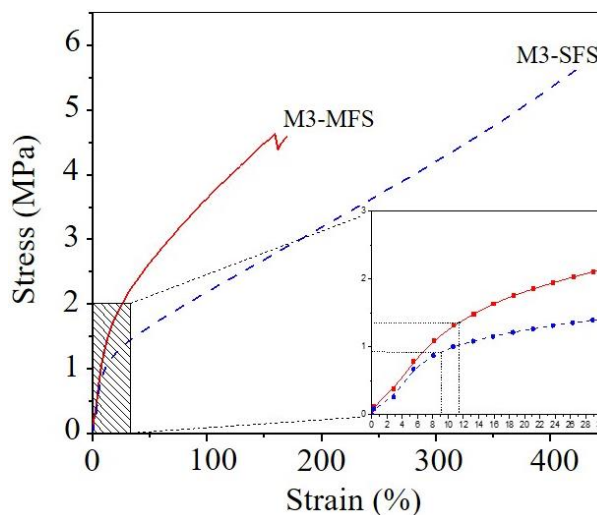


Figure 10 Stress-strain curves of the M3-MFS and M3-SFS under tension loading to the rupture point.

strain level, as shown in Figures 8-10. All models of SFS have similar stress-strain behaviors regardless of their sizes. As for MFS, when ligament thickness increases stress is reduced noticeably. All models of MFS specimens have greater values of Young's Modulus compared with the SFS specimens, as shown in Table 1.

A notable feature due to ligament thickness is that the increase of ligament thickness make the MFS undergoes certain stress drop before reaching full blown rupture at lower stress level. This is illustrated in Figures 8-10, where model 1 undergoes no stress drop. This is the opposite of the compression loading case, which increasing ligament thickness causes higher

Table 1 Young's Modulus of both the MFS and SFS specimens

Model	Young's Modulus (MPa)	
	MFS	SFS
M1	0.1378±0.0091	0.0933±0.0071
M2	0.1361±0.0096	0.0976±0.0053
M3	0.1326±0.0048	0.0983±0.0045

stress [8]. However models 2 and 3 undergo some stress drop. Eventually all models reach full blown rupture at different stress levels. Stress plateau have not been observed in all cases due to the fact that stress rises along with greater tension and stops when full blown rupture takes place. It is also worth noting that increasing ligament thickness reduces tolerable stress level under tension loading whereas under compression loading the opposite has been reported [8].

4. Conclusion

Experimental investigation of mechanical behavior of the MFS under uniaxial tension loading has been performed. Both hysteretic characteristics and stress-strain curves under tension loading are in the same manner as results from compression loading experiments. That is the MFS, a cellular structure material, exhibits larger hysteresis loop than the SFS. When undergoing tension loading to the rupture point the MFS appears with greater stiffness to tension at moderate level of loading compared with the SFS. Both phenomena are likely due to elastic instability present in the MFS but not discernable in the SFS. Finally, it is worth noting that ligament thickness affects the specimens tolerable stress level under tension loading in an opposite direction compared with the compression loading case.

5. Acknowledgment

The authors are thankful to the Rubber and Polymer Technology Program, Faculty of Science and Technology Songkhla Rajabhat University for materials, tools, equipment and space for the experiment. Financial support for this research from Faculty of Engineering, Pathumwan Institute of Technology is also greatly appreciated.

6. References

- [1] Lakes RS. Foam structures with a negative Poisson's ratio. *Science*. 1987;235:1038-40.
- [2] Evans KE, Nkansah MA, Hutchinson IJ, Rogers SC. Molecular network design. *Nature*. 1991;353:124.
- [3] Gibson LJ, Ashby MF. Cellular solids: structure and properties. 2nd ed. Cambridge: Cambridge University Press; 1997.
- [4] Zhang K, Zhao XW, Duan HL, Karihaloo BL, Wang J. Pattern transformations in periodic cellular solids under external stimuli. *J Appl Phys*. 2011;109:084907.
- [5] Ball P. The self-made tapestry: Pattern formation in nature. New York: Oxford University Press; 1999.
- [6] Mullin T, Deschanel S, Bertoldi K, Boyce MC. Pattern transformation triggered by deformation. *Phys Rev Lett*. 2007;99:084301.
- [7] Bertoldi K, Boyce MC. Mechanically triggered transformations of phononic band gaps in periodic elastomeric structures. *Phys Rev B*. 2008; 77:052105.
- [8] Bertoldi K, Boyce MC, Deschanel S, Prangea SM, Mullin T. Mechanics of deformation-triggered pattern transformations and superelastic behavior in periodic elastomeric structures. *J Mech Phys Solid*. 2008;56: 2642-68.
- [9] Kolken HMA, Zadpoor AA. Auxetic mechanical metamaterials. *RSC Adv*. 2017;7:5111-29.
- [10] Launey ME, Buehler MJ, Ritchie RO. On the mechanistic origins of toughness in bone. *Annu Rev Mater Res*. 2010; 40:25-53.
- [11] Wegst UGK, Ashby MF. The mechanical efficiency of natural materials. *Phil Mag*. 2004;84(21):2167-86.
- [12] Zadpoor AA. Mechanical meta-materials. *Mater Horiz*. 2016;3:371-81.
- [13] Yu X, Zhou J, Liang H, Jiang Z, Wu L. Mechanical metamaterials associated with stiffness, rigidity and compressibility: a brief review. *Progr Mater Sci*. 2018;94: 114-73.
- [14] Chen Y, Jia Z, Wang L. Hierarchical honeycomb lattice metamaterials with improved thermal resistance and mechanical properties. *Compos Struct*. 2016;152:395-402.
- [15] Kadic M, Bückmann T, Schittny R, Wegener M. Metamaterials beyond electromagnetism. *Rep Progr Phys*. 2013;76:126501.
- [16] Nicolaou ZG, Motter AE. Mechanical metamaterials with negative compressibility transitions. *Nat Mater*. 2012;11: 608-13.
- [17] Chen BG, Upadhyaya N, Vitelli V. Nonlinear conduction via solutions in a topological mechanical insulator. *PNAS*. 2014;111(36):13004-9.
- [18] Kane CL, Lubensky TC. Topological boundary modes in isostatic lattices. *Nat Phys*. 2014;10:39-45.
- [19] Overvelde JTB, Shan S, Bertoldi K. Compaction through buckling in 2D periodic, soft and porous structures: effect of pore shape. *Adv Mater*. 2012;24(17):2337-42.
- [20] Sanami M, Ravirala N, Alderson K, Alderson A. Auxetic materials for sports applications. *Procedia Eng*. 2014;72: 453-8.
- [21] Bianchi M, Scarpa F, Smith C. Shape memory behavior in auxetic foams: mechanical properties. *Acta Mater*. 2010; 58(3):858-65.
- [22] Lira C, Scarpa F, Rajasekaran R. A gradient cellular core for aeroengine fan blades based on auxetic configurations. *J Intell Mater Syst Struct*. 2011;22(9):907-17.
- [23] Liu Q. Literature review: materials with negative Poisson's ratios and potential applications to aerospace and defence. Australia: Defence Science and Technology Organisation; 2006.
- [24] Santo L. Shape memory polymer foams. *Progr Aero Sci*. 2016;81:60-5.
- [25] Scarpa F. Auxetic materials for bioprotheses. *IEEE Signal Process Mag*. 2008;25(5):128-26.
- [26] Bertoldi K, Reis PM, Willshaw S, Mullin T. Negative Poisson's ratio behavior induced by an elastic instability. *Adv Mater*. 2010;22:361-6.
- [27] Chen Y, Jin L. Geometric role in designing pneumatically actuated pattern-transforming metamaterials. *Extreme Mech Lett*. 2018;23:55-66
- [28] Wang P, Shim J, Bertoldi K. Effects of geometric and material non-linearities on the tunable bandgaps and low-frequency directionality of phononic crystals. *Phys Rev B*. 2013;88:014304.
- [29] Florijn B, Coulaissab C, Heckeb MV. Programmable mechanical metamaterials: the role of geometry. *Soft Matter*. 2016;12:8736-43.
- [30] ABAQUS. Analysis User's Manual Version 6.5. USA: Hibbitt Karlsson & Sorensen Inc; 2005.

- [31] Halzapfel GA, Stadler M, Ogden RW. Aspect of stress softening in filled rubbers incorporating residual strain. In: Dorfmann A, Muhr A, editors. Constitutive Models for Rubber. Rotterdam: CRC Press; 1999. p. 189-13.
- [32] Florijn B, Coulais C, Hecke MV. Programmable mechanical metamaterials. *Phys Rev Lett*. 2014;113:17-24.
- [33] Gent AN. *Engineering with rubber*. 2nd ed. New York: Oxford University Press; 1992.
- [34] Ronald J. Dynamics properties of rubber. *Rubber World*. 1994;211:43-5.
- [35] Zheng X, Lee H, Weisgraber TH, Shusteff M, DeOtte J, Duoss EB, et al. Ultralight, ultrastiff mechanical metamaterials. *Science*. 2014;344:1373-7.
- [36] Meza LR, Das S, Greer JR. Strong, lightweight, and recoverable three-dimensional ceramic nanolattices. *Science*. 2014;345:1322-6.